Supporting Information

Solubility of Water in Hydrogen at High Pressures: A Molecular Simulation Study

Ahmadreza Rahbari,[†] Jeroen Brenkman,[‡] Remco Hens,[†] Mahinder Ramdin,[†] Leo J. P. van den Broeke,[†] Rogier Schoon,[‡] Ruud Henkes,[‡] Othonas A. Moultos,[†] and Thijs J. H. Vlugt[*,†]

[†]*Engineering Thermodynamics, Process & Energy Department, Faculty of Mechanical, Maritime and Materials Engineering, Delft University of Technology, Leeghwaterstraat 39, 2628CB, Delft, The Netherlands*

[‡]*Shell Global Solutions International, PO Box 38000, 1030BN, Amsterdam, the Netherlands*

E-mail: t.j.h.vlugt@tudelft.nl

Fugacity Coefficients

Consider a multicomponent system that is simulated in an ensemble that is either open (e.g. grand-canonical ensemble) or closed (NPT ensemble). In this system, we would like to calculate the fugacity coefficient ϕ_i of component i. We assume that a fractional molecule of component i is present. The chemical potential of component i equals[1,2]

$$\mu_i = \mu_i^0 + RT \ln \frac{\langle \rho_i \rangle}{\rho_0} + \mu_{\text{ex}}^i = \mu_i^0 + RT \ln \frac{\langle \rho_i \rangle}{\rho_0} - RT \ln \frac{p(\lambda_i = 1)}{p(\lambda_i = 0)} \tag{S1}$$

in which μ_i^0 is the reference state of the chemical potential, $\langle \rho_i \rangle$ is the average number density of i, μ_{ex}^i is the excess chemical potential of i, ρ_0 is an arbitrary reference density (to make the argument of the logarithm dimensionless), and $p(\lambda_i)$ is the (unbiased) Boltzmann probability distribution of the coupling parameter of the fractional molecule of type i. In classical thermodynamics, the chemical potential of i is usually expressed as[3,4]

$$\mu_i = \mu_i^\star + RT \ln \left(\frac{y_i P \phi_i}{P_0} \right) \tag{S2}$$

in which $\mu_i^\star$ is a reference chemical potential (which is different from μ_i^0), y_i is the mole fraction of i, P is the pressure, and P_0 is a reference pressure (usually 1 bar). The reference chemical potentials μ_i^0 and $\mu_i^\star$ only depend on the temperature and not on the pressure or composition of the system. To find an expression for the fugacity coefficient ϕ_i, consider a system in which the pressure P is approaching zero while the composition of the mixture is constant. In this limit, $\phi_i = 1$ and $\mu_{\text{ex}}^i = 0$. We have

$$\mu_i^0 + RT \ln \frac{\langle \rho_i \rangle}{\rho_0} = \mu_i^\star + RT \ln \left(\frac{y_i P}{P_0} \right) \tag{S3}$$

In this limit, the ideal gas law can also be used to calculate the average number density of i,

$$\langle \rho_i \rangle = \frac{y_i P}{RT} \tag{S4}$$

This leads to

$$\mu_i^0 - \mu_i^\star = RT \ln \left(\frac{\rho_0 RT}{P_0} \right) \tag{S5}$$

This equation can be used to eliminate the reference state in Eq. S2 leading to

$$\mu_{\text{ex}}^i = RT \ln \left(\frac{y_i P \phi_i}{RT \langle \rho_i \rangle} \right) \tag{S6}$$

so

$$\phi_i = \frac{RT \langle \rho_i \rangle}{y_i P} \exp \left[\mu_{\text{ex}}^i / (RT) \right] \tag{S7}$$

If the system consists of N_t molecules in total (including component i, and not counting fractional molecules), we have $\langle \rho_i \rangle \approx N_i / \langle V \rangle$ ($\langle V \rangle$ being the average volume) and $y_i = N_i / N_t$. Finally, we have

$$\phi_i = \frac{N_t RT}{P \langle V \rangle} \exp \left[\mu_{\text{ex}}^i / (RT) \right] = \frac{\exp \left[\mu_{\text{ex}}^i / (RT) \right]}{Z_m} \tag{S8}$$

in which $Z_m = \frac{P \langle V \rangle}{N_t RT}$ is the compressibility of the mixture. The fugacity coefficient ϕ_i thus depends on both the excess chemical potential of i and the overall deviation from ideal gas behavior of the mixture.

Equation of State Modelling

The condition of equilibrium between the gas and liquid phase requires equal chemical potentials (*i.e.* equal fugacities) for both phases at a certain temperature and pressure. At any set of T and P, the fugacity of component i in the liquid phase can be defined using the activity coefficient.[5] The fugacity of component i in the gas phase can be calculated using an equation of state. By equating the fugacities, we have[5]

$$\varphi_i y_i P = \gamma_i x_i \phi_i^{\text{sat}} P_i^{\text{sat}} \exp\left[\frac{V_i^{\text{L}}\left(P - P_i^{\text{sat}}\right)}{RT}\right] \tag{S9}$$

where φ_i and y_i are the fugacity coefficient and mole fraction of component i in the gas phase, respectively. This equation resembles the $\gamma - \phi$ approach. γ_i and x_i are the activity coefficient and mole fraction of component i in the liquid phase, respectively. V_i^{L} and P_i^{sat} are the molar volume and saturation pressure of the liquid at temperature T. The exponential term on the right hand side of Eq. S9 is the Poynting factor, which accounts for changes in the chemical potential due to the compressibility of the liquid. At ambient pressures this term is close to 1, but at the pressures in this study (100-1000 bar) this term significantly differs from 1. For the $H_2O - H_2$ system at high pressures, it is known that the liquid phase contains almost pure water, and the gas phase contains almost pure hydrogen. Therefore, the mole fraction of water in the gas phase can be calculated easily by simplifying Eq. S9. γ_i and x_i for water in the liquid phase can be set to one since the liquid phase is almost pure water. The activity coefficient of water in the gas phase can be estimated at infinite dilution since the mole fraction of water is significantly low in the gas phase. Other parameters in Eq. S9 can be obtained from pure component data.[6] The drawback of this method is that the composition of the liquid phase remains unknown. One can use flash calculations to predict the vaporized fraction of the mixture as well as the liquid composition in equilibrium. The fugacity coefficients at (T, P) are calculated from an EoS in every iteration to compute

the distribution coefficient.[5,7] The flash calculations (ϕ-ϕ approach) were performed using the software by Martín and co-workers.[8] For details the reader is referred to Ref.[8]

Table S1: Force field parameters for the water models used in this study. L is the dummy site for four-site models. For the TIP5P/Ew[9] model, L and M are the dummy sites. θ is the angle between atoms OHO, in degrees. For four-site water models $\varepsilon = 0.5\theta$. φ is the angle between the point charges of the dummy sites for the TIP5P/Ew. A cutoff radius of 12 Å was used for all LJ interactions. Analytic tail corrections and the Lorentz-Berthelot mixing rules were applied.[10,11]

Force Field Parameters	TIP3P[12]	SPC[13]	SPC/E[14]	OPC[15]	TIP4P/2005[16]	TIP4P/Ew[17]	TIP5P/Ew[9]
$\epsilon_{OO}/k_B/[K]$	76.500	78.203	78.175	107.086	93.196	81.899	89.57888
$\sigma_{OO}/[\text{Å}]$	3.151	3.1656	3.166	3.1666	3.1589	3.1644	3.097
$q_O/[e]$	-0.834	-0.82	-0.8476	-1.3582	-		-
$q_H/[e]$	0.417	0.41	0.4238	0.6791	0.5564	0.52422	-
$q_L/[e]$	-	-	-	-1.3582	-1.1128	-1.04844	-0.241
$q_M/[e]$	-	-	-	-	-	-	0.241
$r_{OH}/[\text{Å}]$	0.957		1	0.8724	0.9572	0.9572	
$r_{OL}/[\text{Å}]$	-	-	-	0.1594	0.1546	0.125	
θ	104.52	109.47	109.47	103.6	104.52	104.52	104.52
φ	-	-	-	51.8	52.26	52.26	109.47

Table S2: Force field parameters for the hydrogen models used in this study. Dummy site L is the geometric center of mass for the Marx model. The H-H bond length of the two-site and three-site force fields is 0.74 Å. A cutoff radius of 12 Å was used for all LJ interactions. Analytic tail corrections and the Lorentz-Berthelot mixing rules were applied.[10,11]

Force Field Parameters	Buch[18]	Hirschfelder[19]	Vrabec[20]	Cracknell[21]	Marx[22]
$\epsilon_{HH}/k_B/[K]$	34.2	38	25.84	12.5	-
$\sigma_{HH}/[Å]$	2.96	2.915	3.0366	2.59	-
$q_H/[e]$	-	-	-	-	0.468
$q_L/[e]$	-	-	-	-	-0.936
$\epsilon_{LL}/k_B/[K]$	-	-	-	-	36.7
$\sigma_{LL}/[Å]$	-	-	-	-	2.958

Table S3: Calculated densities and fugacity coefficients of different hydrogen models obtained from CFC*NPT* simulations at $T = 323$ K and pressures between $P = 100$ and $P = 1000$ bar. The results from equation of state modelling are obtained using parameters from table S10. σ_x is the uncertainty of x. Results from cubic EoS and REFPROP[23,24] are also included.

$P/[\text{bar}]$	$\langle\rho\rangle/[\text{kg/m}^3]$	$\sigma_{\langle\rho\rangle}$	$\mu/k_{\text{B}}/[\text{K}]$	σ_ϕ
Hirschfelder[19]				
100	7.121	0.001	1.05	0.02
200	13.556	0.002	1.10	0.02
400	24.650	0.006	1.23	0.02
600	33.84	0.01	1.37	0.03
800	41.58	0.01	1.53	0.03
1000	48.22	0.02	1.71	0.03
Vrabec[20]				
100	7.027	0.001	1.06	0.02
200	13.239	0.002	1.14	0.02
400	23.733	0.005	1.30	0.02
600	32.30	0.01	1.48	0.02
800	39.49	0.01	1.67	0.03
1000	45.65	0.01	1.92	0.03
Buch[18]				
100	7.088	0.001	1.05	0.02
200	13.443	0.003	1.12	0.02
400	24.314	0.006	1.25	0.02
600	33.26	0.01	1.40	0.02
800	40.78	0.01	1.59	0.02
1000	47.22	0.01	1.79	0.03
Cracknell[21]				
100	7.133	0.001	1.05	0.02
200	13.611	0.003	1.10	0.02
400	24.891	0.005	1.21	0.02
600	34.37	0.01	1.35	0.02
800	42.45	0.01	1.50	0.03
1000	49.45	0.01	1.66	0.03
Marx[22]				
100	7.100	0.002	1.05	0.02
200	13.482	0.004	1.11	0.02
400	24.416	0.010	1.25	0.02
600	33.41	0.02	1.40	0.03
800	40.97	0.02	1.57	0.03
1000	47.42	0.02	1.76	0.04

$P/[\text{bar}]$	$\langle\rho\rangle/[\text{kg/m}^3]$	$\sigma_{\langle\rho\rangle}$	$\mu/k_{\text{B}}/[\text{K}]$	σ_ϕ
PR-EoS [25]				
100	7.35	-	1.03	-
200	14.05	-	1.07	-
400	25.60	-	1.17	-
600	35.00	-	1.28	-
800	42.73	-	1.42	-
1000	49.17	-	1.57	-
SRK-EoS [26]				
100	7.19	-	1.05	-
200	13.58	-	1.11	-
400	24.36	-	1.25	-
600	33.00	-	1.41	-
800	40.04	-	1.60	-
1000	45.87	-	1.82	-
REFPROP [23,24]				
100	7.10	-	1.06	-
200	13.46	-	1.12	-
400	24.29	-	1.26	-
600	33.17	-	1.42	-
800	40.63	-	1.60	-
1000	47.01	-	1.80	-

Table S4: Calculated densities and chemical potentials of different water models obtained from CFC*NPT* simulations at $T = 323$ K and pressures between $P = 100$ and $P = 1000$ bar. σ_x is the uncertainty of x. Results from REFPROP[23,24] are also included.

$P/[\mathrm{bar}]$	$\langle\rho\rangle/[\mathrm{kg/m^3}]$	$\sigma_{\langle\rho\rangle}$	$\mu/k_\mathrm{B}/[\mathrm{K}]$	σ_μ
	TIP3P[13]			
100	965	2	-4057	31
200	970	1	-4033	25
400	982	2	-3989	32
600	992	1	-3948	29
800	1002	1	-3905	30
1000	1011	1	-3861	25
	SPC[12]			
100	962	2	-4075	24
300	973	2	-4021	32
500	982	1	-3987	26
800	996	2	-3912	29
1000	1005	1	-3873	28
	SPC/E[14]			
100	987	2	-4482	36
300	997	1	-4424	33
500	1004	2	-4385	31
800	1017	2	-4311	42
1000	1025	2	-4271	42
	TIP4P/2005[16]			
100	990	2	-4606	47
200	995	2	-4584	44
400	1003	2	-4554	49
600	1012	2	-4494	48
800	1020	2	-4467	55
1000	1027	2	-4408	45
	TIP4P/Ew[17]			
100	987	2	-4433	35
300	996	2	-4388	25
500	1006	1	-4355	38
800	1018	2	-4291	41
1000	1025	2	-4242	38
	OPC[15]			
100	991	2	-4946	38
300	998	2	-4902	52
500	1005	2	-4861	43

Continued on next page

P/[bar]	$\langle\rho\rangle$/[kg/m^3]	$\sigma_{\langle\rho\rangle}$	μ/k_{B}/[K]	σ_μ
800	1017	2	-4808	59
1000	1025	2	-4730	61
TIP5P/Ew[9]				
100	990	2	-3845	24
300	1000	1	-3821	24
500	1011	2	-3769	27
800	1025	2	-3699	30
1000	1034	2	-3651	29
REFPROP[23,27]				
100	992.31	-	-4112.58	-
200	996.53	-	-4089.42	-
400	1004.7	-	-4043.47	-
600	1012.6	-	-3997.99	-
800	1020.1	-	-3952.96	-
1000	1027.4	-	-3908.32	-

Table S5: Experimental solubilities of hydrogen in $H_2O - H_2$ mixtures (liquid phase) at coexistence. Experimental data are converted to mole fractions for different temperatures and pressures. For the original units for each data set, see the indicated references below. For conversion to mole fractions, standard conditions at $T = 273.15$ K and $P = 1.01325$ atm are considered, unless otherwise stated in the reference.

T/[K]	P/[bar]	x_{H_2}	Ref.
273.15	25	4.31×10^{-4}	[28]
273.15	51	8.63×10^{-4}	[28]
273.15	101	1.71×10^{-3}	[28]
273.15	203	3.35×10^{-3}	[28]
273.15	405	6.40×10^{-3}	[28]
273.15	608	9.25×10^{-3}	[28]
273.15	811	1.19×10^{-2}	[28]
273.15	1013	1.42×10^{-2}	[28]
298.15	25	3.50×10^{-4}	[28]
298.15	51	6.94×10^{-4}	[28]
298.15	101	1.39×10^{-3}	[28]
298.15	203	2.71×10^{-3}	[28]
298.15	405	5.24×10^{-3}	[28]
298.15	608	7.64×10^{-3}	[28]
298.15	811	9.90×10^{-3}	[28]
298.15	1013	1.20×10^{-2}	[28]
310.15	1.013	1.33×10^{-5}	[29]
310.93	3.4	4.50×10^{-5}	[30]
310.93	13.8	1.81×10^{-4}	[30]
310.93	31.0	4.10×10^{-4}	[30]
310.93	65.5	8.62×10^{-4}	[30]
310.93	103.4	1.33×10^{-3}	[30]
310.93	137.9	1.76×10^{-3}	[30]
323.15	25	3.26×10^{-4}	[28]
323.15	31.8	4.02×10^{-4}	[31]
323.15	51	6.49×10^{-4}	[28]
323.15	60.3	7.63×10^{-4}	[31]
323.15	101	1.29×10^{-3}	[28]
323.15	119.3	1.51×10^{-3}	[31]
323.15	203	2.54×10^{-3}	[28]
323.15	405	4.92×10^{-3}	[28]
323.15	608	7.18×10^{-3}	[28]
323.15	811	9.34×10^{-3}	[28]
323.15	1013	1.14×10^{-2}	[28]
348.15	25	3.32×10^{-4}	[28]
348.15	51	6.63×10^{-4}	[28]
348.15	101	1.32×10^{-3}	[28]

Continued on next page

T/[K]	P/[bar]	x_{H_2}	Ref.
348.15	203	2.60×10^{-3}	[28]
348.15	405	5.04×10^{-3}	[28]
348.15	608	7.35×10^{-3}	[28]
348.15	811	9.54×10^{-3}	[28]
348.15	1013	1.17×10^{-2}	[28]
366.48	3.4	3.74×10^{-5}	[30]
366.48	13.8	2.0×10^{-4}	[32]
366.48	13.8	1.80×10^{-4}	[30]
366.48	27.6	3.7×10^{-4}	[32]
366.48	31.0	4.26×10^{-4}	[30]
366.48	55.2	7.5×10^{-4}	[32]
366.48	65.5	8.93×10^{-4}	[30]
366.48	110.3	1.50×10^{-3}	[32]
366.48	137.9	1.840×10^{-3}	[30]
373.15	21	3.01×10^{-4}	[33]
373.15	25	3.70×10^{-4}	[28]
373.15	31	4.48×10^{-4}	[33]
373.15	42	5.94×10^{-4}	[33]
373.15	42	5.17×10^{-4}	[34]
373.15	51	7.30×10^{-4}	[28]
373.15	57.0	8.20×10^{-4}	[31]
373.15	62	8.77×10^{-4}	[33]
373.15	62	7.61×10^{-4}	[34]
373.15	82	1.15×10^{-3}	[33]
373.15	82	1.02×10^{-3}	[34]
373.15	101	1.45×10^{-3}	[28]
373.15	102	1.32×10^{-3}	[34]
373.15	120.9	1.75×10^{-3}	[31]
373.15	153.7	2.23×10^{-3}	[31]
373.15	203	2.85×10^{-3}	[28]
373.15	405	5.46×10^{-3}	[28]
373.15	608	7.96×10^{-3}	[28]
373.15	811	1.03×10^{-2}	[28]
373.15	1013	1.25×10^{-2}	[28]
398.15	23	3.44×10^{-4}	[33]
398.15	33	5.04×10^{-4}	[33]
398.15	43	6.54×10^{-4}	[33]
398.15	52	7.18×10^{-4}	[34]
398.15	63	9.32×10^{-4}	[33]
398.15	82	1.13×10^{-3}	[34]
398.15	83	1.21×10^{-3}	[33]
398.15	87	1.21×10^{-3}	[34]
398.15	102	1.43×10^{-3}	[34]

$T/[\text{K}]$	$P/[\text{bar}]$	x_{H_2}	Ref.
422.04	31.0	5.00×10^{-4}	[30]
422.04	65.5	1.16×10^{-3}	[30]
422.04	103.4	1.88×10^{-3}	[30]
423.15	21	3.26×10^{-4}	[33]
423.15	30	4.95×10^{-4}	[33]
423.15	31	4.370×10^{-4}	[34]
423.15	40	6.55×10^{-4}	[33]
423.15	42	5.98×10^{-4}	[34]
423.15	52	7.79×10^{-4}	[34]
423.15	51.8	9.00×10^{-4}	[31]
423.15	54.3	9.79×10^{-4}	[31]
423.15	55	8.75×10^{-4}	[33]
423.15	62	9.43×10^{-4}	[34]
423.15	76	1.15×10^{-3}	[33]
423.15	75.9	1.35×10^{-3}	[31]
423.15	82	1.34×10^{-3}	[34]
423.15	87.1	1.60×10^{-3}	[31]
448.15	22	3.28×10^{-4}	[33]
448.15	29	4.83×10^{-4}	[33]
448.15	39	6.59×10^{-4}	[33]
448.15	52	7.46×10^{-4}	[34]
448.15	60	9.56×10^{-4}	[33]
448.15	62	9.43×10^{-4}	[34]
448.15	80	1.24×10^{-3}	[33]
473.15	26	3.30×10^{-4}	[33]
473.15	31	1.00×10^{-3}	[33]
473.15	36	5.74×10^{-4}	[33]
473.15	42	5.52×10^{-4}	[34]
473.15	46	8.44×10^{-4}	[33]
473.15	52	7.51×10^{-4}	[34]
473.15	76	1.22×10^{-3}	[33]
473.15	82	1.24×10^{-3}	[34]
473.15	102	1.40×10^{-3}	[34]
473.15	118	1.62×10^{-3}	[34]
477.59	27.6	3.5×10^{-4}	[32]
477.59	31.0	4.29×10^{-4}	[30]
477.59	55.2	1.05×10^{-3}	[32]
477.59	65.5	1.46×10^{-3}	[30]
477.59	103.4	2.57×10^{-3}	[30]
477.59	110.3	2.71×10^{-3}	[32]
498.15	33	3.22×10^{-4}	[33]
498.15	36	4.47×10^{-4}	[33]
498.15	41	5.91×10^{-4}	[33]

$T/[\text{K}]$	$P/[\text{bar}]$	x_{H_2}	Ref.
498.15	51	8.10×10^{-4}	[33]
498.15	62	9.93×10^{-4}	[34]
498.15	71	1.21×10^{-3}	[33]
498.15	92	1.45×10^{-3}	[34]
523.15	44	2.70×10^{-4}	[33]
523.15	47	4.45×10^{-4}	[33]
523.15	52	6.50×10^{-4}	[33]
523.15	60	8.93×10^{-4}	[33]
523.15	70	1.18×10^{-3}	[33]
548.15	63	3.01×10^{-4}	[33]
548.15	65	4.70×10^{-4}	[33]
548.15	68	6.54×10^{-4}	[33]
548.15	72	8.48×10^{-4}	[33]
548.15	80	1.19×10^{-3}	[33]
573.15	89	2.86×10^{-4}	[33]
573.15	91	5.42×10^{-4}	[33]
573.15	93	7.24×10^{-4}	[33]
573.15	96	8.80×10^{-4}	[33]
573.15	100	1.25×10^{-3}	[33]
574.81	110.3	1.41×10^{-3}	[32]
588.70	110.3	2.26×10^{-3}	[32]
588.71	137.9	2.98×10^{-3}	[30]

Table S6: Experimental solubilities of water in $H_2O - H_2$ mixtures (gas phase) at coexistence. Experimental data are converted to mole fractions for different temperatures and pressures. For the original units for each data set, see the references below. For conversion to mole fractions, standard conditions at $T = 273.15$ K and $P = 1.01325$ atm are considered, unless otherwise stated in the reference.

$T/[K]$	$P/[bar]$	x_{H_2}	Ref.
310.93	3.4	1.96×10^{-2}	30
310.93	13.8	4.88×10^{-3}	30
310.93	31.0	2.22×10^{-3}	30
310.93	65.5	1.16×10^{-3}	30
310.93	103.4	7.6×10^{-4}	30
310.93	137.9	6.0×10^{-4}	30
310.95	13.8	4.88×10^{-3}	35
310.95	31.0	2.22×10^{-3}	35
310.95	65.5	1.16×10^{-3}	35
310.95	103.4	7.60×10^{-4}	35
323.15	50	2.66×10^{-3}	36
323.15	100	1.48×10^{-3}	36
323.15	101.3	1.38×10^{-3}	37
323.15	150	1.08×10^{-3}	36
323.15	200	8.8×10^{-4}	36
323.15	202.7	7.84×10^{-4}	37
323.15	250	7.6×10^{-4}	36
323.15	300	6.8×10^{-4}	36
323.15	405.3	4.64×10^{-4}	37
323.15	608.0	3.61×10^{-4}	37
323.15	1013.3	2.80×10^{-4}	37
343.15	50	6.60×10^{-3}	36
343.15	100	3.58×10^{-3}	36
343.15	150	2.57×10^{-3}	36
343.15	200	2.07×10^{-3}	36
343.15	250	1.77×10^{-3}	36
343.15	300	1.57×10^{-3}	36
366.45	13.8	3.86×10^{-3}	35
366.45	31.0	2.64×10^{-3}	35
366.45	65.5	1.32×10^{-3}	35
366.45	137.9	6.68×10^{-3}	35
366.48	3.4	2.47×10^{-1}	30
366.48	13.8	5.54×10^{-2}	32
366.48	13.8	5.86×10^{-2}	30
366.48	27.6	3.08×10^{-2}	32
366.48	31.0	2.64×10^{-2}	30
366.48	55.2	1.63×10^{-2}	32

Continued on next page

T/[K]	P/[bar]	y_{H_2O}	Ref.
366.48	65.5	1.32×10^{-2}	[30]
366.48	110.3	6.51×10^{-3}	[32]
366.48	137.9	6.68×10^{-3}	[30]
422.04	31.0	1.570×10^{-1}	[30]
422.04	65.5	7.53×10^{-2}	[30]
422.04	103.4	5.13×10^{-2}	[30]
423.15	50	1.06×10^{-1}	[36]
423.15	100	6.00×10^{-2}	[36]
423.15	150	4.40×10^{-2}	[36]
423.15	200	3.60×10^{-2}	[36]
423.15	250	3.12×10^{-2}	[36]
423.15	300	2.83×10^{-2}	[36]
448.15	50	2.06×10^{-1}	[36]
448.15	100	1.21×10^{-1}	[36]
448.15	150	9.27×10^{-2}	[36]
448.15	200	7.80×10^{-2}	[36]
448.15	250	6.88×10^{-2}	[36]
448.15	300	6.23×10^{-2}	[36]
473.15	50	2.66×10^{-1}	[36]
473.15	100	1.48×10^{-1}	[36]
473.15	150	1.08×10^{-1}	[36]
473.15	200	8.8×10^{-2}	[36]
473.15	250	7.6×10^{-2}	[36]
473.15	300	6.9×10^{-2}	[36]
477.59	27.6	6.34×10^{-1}	[32]
477.59	31.0	5.55×10^{-1}	[30]
477.59	55.2	3.26×10^{-1}	[32]
477.59	65.5	2.85×10^{-1}	[30]
477.59	103.4	1.88×10^{-1}	[30]
477.59	110.3	1.72×10^{-1}	[32]
498.15	50	5.54×10^{-1}	[36]
498.15	100	3.22×10^{-1}	[36]
498.15	150	2.44×10^{-1}	[36]
498.15	200	2.08×10^{-1}	[36]
498.15	250	1.83×10^{-1}	[36]
498.15	300	1.67×10^{-1}	[36]
523.15	50	8.26×10^{-1}	[36]
523.15	100	4.96×10^{-1}	[36]
523.15	150	3.83×10^{-1}	[36]
523.15	200	3.27×10^{-1}	[36]
523.15	250	2.94×10^{-1}	[36]
523.15	300	2.71×10^{-1}	[36]
548.15	100	6.86×10^{-1}	[36]

Continued on next page

T/[K]	P/[bar]	$y_{\text{H}_2\text{O}}$	Ref.
548.15	150	5.36×10^{-1}	[36]
548.15	200	4.61×10^{-1}	[36]
548.15	250	4.16×10^{-1}	[36]
548.15	300	3.86×10^{-1}	[36]
573.15	100	9.00×10^{-1}	[36]
573.15	150	7.22×10^{-1}	[36]
573.15	200	6.33×10^{-1}	[36]
573.15	250	5.82×10^{-1}	[36]
573.15	300	5.51×10^{-1}	[36]
574.81	110.3	8.45×10^{-1}	[32]
588.7	110.3	9.67×10^{-1}	[32]
588.71	137.9	8.10×10^{-1}	[30]

Table S7: Computed compositions of $H_2O - H_2$ mixtures at coexistence using MC simulations. x_{H_2} is the mole fraction of hydrogen in the liquid phase, y_{H_2O} is the mole fraction of water in the gas phase. The $H_2O - H_2$ mixture is defined by the TIP3P[13]-Marx[22] force fields. The simulation techniques are described in the main text. σ_x is the uncertainty of x.

T/[K]	P/[bar]	x_{H_2}/[−]	$\sigma_{x_{H_2}}$	y_{H_2O}/[−]	$\sigma_{y_{H_2O}}$	Sim. Tech.
283	10	1.510×10^{-4}	9×10^{-7}	1.8×10^{-3}	1×10^{-4}	CFC*NPT*
283	50	7.48×10^{-4}	6×10^{-6}	3.7×10^{-4}	3×10^{-5}	CFC*NPT*
283	80	1.174×10^{-3}	8×10^{-6}	2.4×10^{-4}	2×10^{-5}	CFC*NPT*
283	100	1.47×10^{-3}	1×10^{-5}	2.0×10^{-4}	1×10^{-5}	CFC*NPT*
283	300	4.28×10^{-3}	4×10^{-5}	7.3×10^{-5}	5×10^{-6}	CFC*NPT*
283	500	6.79×10^{-3}	7×10^{-5}	4.8×10^{-5}	4×10^{-6}	CFC*NPT*
283	800	9.51×10^{-3}	9×10^{-5}	3.5×10^{-5}	2×10^{-6}	CFC*NPT*
283	1000	1.162×10^{-2}	9×10^{-5}	2.9×10^{-5}	4×10^{-6}	CFC*NPT*
310	10	1.6×10^{-4}	2×10^{-5}	9.3×10^{-3}	8×10^{-4}	GE
310	50	8.1×10^{-4}	8×10^{-5}	2.3×10^{-3}	4×10^{-4}	GE
310	80	1.29×10^{-3}	9×10^{-5}	1.3×10^{-3}	5×10^{-4}	GE
310	100	1.6×10^{-3}	1×10^{-4}	1.2×10^{-3}	3×10^{-4}	GE
310	100	1.64×10^{-3}	2×10^{-5}	9.8×10^{-4}	7×10^{-5}	CFC*NPT*
310	300	4.59×10^{-3}	9×10^{-5}	3.5×10^{-4}	4×10^{-5}	CFC*NPT*
310	500	7.3×10^{-3}	1×10^{-4}	2.4×10^{-4}	5×10^{-5}	CFC*NPT*
310	800	1.08×10^{-2}	2×10^{-4}	1.7×10^{-4}	4×10^{-5}	CFC*NPT*
310	1000	1.31×10^{-2}	2×10^{-4}	1.4×10^{-4}	5×10^{-5}	CFC*NPT*
323	10	1.7×10^{-4}	1×10^{-5}	1.74×10^{-2}	1×10^{-3}	GE
323	50	8.8×10^{-4}	7×10^{-5}	3.57×10^{-3}	7×10^{-4}	GE
323	80	1.4×10^{-3}	1×10^{-4}	2.35×10^{-3}	6×10^{-4}	GE
323	100	1.7×10^{-3}	1×10^{-4}	2.00×10^{-3}	4×10^{-4}	GE
323	300	4.8×10^{-3}	4×10^{-4}	6.89×10^{-4}	2×10^{-4}	GE
323	500	7.6×10^{-3}	6×10^{-4}	4.45×10^{-4}	2×10^{-4}	GE
323	800	1.14×10^{-2}	8×10^{-4}	3.12×10^{-4}	1×10^{-4}	GE
323	1000	1.4×10^{-2}	1×10^{-3}	3.04×10^{-4}	1×10^{-4}	GE
323	100	1.72×10^{-3}	2×10^{-5}	1.8×10^{-3}	1×10^{-4}	CFC*NPT*
323	300	4.90×10^{-3}	5×10^{-5}	6.4×10^{-4}	8×10^{-5}	CFC*NPT*
323	500	7.7×10^{-3}	1×10^{-4}	4.2×10^{-4}	7×10^{-5}	CFC*NPT*
323	800	1.15×10^{-2}	3×10^{-4}	3.1×10^{-4}	6×10^{-5}	CFC*NPT*
323	1000	1.35×10^{-2}	2×10^{-4}	2.6×10^{-4}	6×10^{-5}	CFC*NPT*
366	10	2.1×10^{-4}	1×10^{-5}	1.08×10^{-1}	7×10^{-3}	GE
366	50	1.16×10^{-3}	5×10^{-5}	2.2×10^{-2}	2×10^{-3}	GE
366	80	1.86×10^{-3}	8×10^{-5}	1.41×10^{-1}	9×10^{-4}	GE
366	100	2.28×10^{-3}	8×10^{-5}	1.14×10^{-1}	6×10^{-4}	GE
366	300	6.4×10^{-3}	3×10^{-4}	4.2×10^{-1}	5×10^{-4}	GE
366	500	1.03×10^{-2}	6×10^{-4}	2.7×10^{-1}	4×10^{-4}	GE
366	800	1.49×10^{-2}	7×10^{-4}	1.8×10^{-1}	4×10^{-4}	GE

Continued on next page

$T/[\text{K}]$	$P/[\text{bar}]$	$x_{\text{H}_2}/[-]$	$\sigma_{x_{\text{H}_2}}$	$y_{\text{H}_2\text{O}}/[-]$	$\sigma_{y_{\text{H}_2\text{O}}}$	Sim. Tech.
366	1000	1.80×10^{-2}	9×10^{-4}	1.4×10^{-1}	4×10^{-4}	GE
423	50	1.70×10^{-3}	5×10^{-5}	1.38×10^{-1}	6×10^{-3}	GE
423	80	2.85×10^{-3}	9×10^{-5}	8.6×10^{-2}	4×10^{-3}	GE
423	100	3.5×10^{-3}	1×10^{-4}	7.2×10^{-2}	3×10^{-3}	GE
423	300	1.03×10^{-2}	4×10^{-4}	2.5×10^{-2}	1×10^{-3}	GE
423	500	1.62×10^{-2}	6×10^{-4}	1.58×10^{-2}	8×10^{-4}	GE
423	800	2.35×10^{-2}	9×10^{-4}	1.02×10^{-2}	5×10^{-4}	GE
423	1000	2.8×10^{-2}	1×10^{-3}	8.2×10^{-3}	6×10^{-4}	GE

Table S8: Computed compositions of $H_2O - H_2$ mixtures at coexistence using MC simulations. x_{H_2} is the mole fraction of hydrogen in the liquid phase, y_{H_2O} is the mole fraction of water in the gas phase. The $H_2O - H_2$ mixture is defined by the TIP4P/2005[16]-Marx[22] force fields. σ_x is the uncertainty of x.

T/[K]	P/[bar]	x_{H_2}/[−]	$\sigma_{x_{H_2}}$	y_{H_2O}/[−]	$\sigma_{y_{H_2O}}$	Sim. Tech.
323	10	1.2×10^{-4}	1×10^{-5}	3.6×10^{-3}	6×10^{-4}	GE
323	50	5.9×10^{-4}	9×10^{-5}	9×10^{-4}	5×10^{-4}	GE
323	80	9.1×10^{-4}	9×10^{-5}	6×10^{-4}	4×10^{-4}	GE
323	100	1.2×10^{-3}	1×10^{-4}	5×10^{-4}	4×10^{-4}	GE
323	300	3.3×10^{-3}	4×10^{-4}	2×10^{-4}	1×10^{-4}	GE
323	500	5.3×10^{-3}	5×10^{-4}	1×10^{-4}	1×10^{-4}	GE
323	800	8.0×10^{-3}	1×10^{-3}	1×10^{-4}	1×10^{-4}	GE
323	1000	1.0×10^{-4}	1×10^{-3}	8×10^{-5}	1×10^{-4}	GE
366	10	1.3×10^{-4}	1×10^{-5}	2.8×10^{-2}	2×10^{-3}	GE
366	50	6.6×10^{-4}	4×10^{-5}	5.8×10^{-3}	5×10^{-4}	GE
366	80	1.0×10^{-3}	6×10^{-5}	3.8×10^{-3}	5×10^{-4}	GE
366	100	1.27×10^{-3}	8×10^{-5}	3.3×10^{-3}	5×10^{-4}	GE
366	300	3.6×10^{-3}	3×10^{-4}	1.2×10^{-3}	5×10^{-4}	GE
366	500	5.9×10^{-3}	6×10^{-4}	9×10^{-4}	4×10^{-4}	GE
366	800	8.7×10^{-3}	8×10^{-4}	5×10^{-4}	3×10^{-4}	GE
366	1000	1.02×10^{-2}	8×10^{-4}	4×10^{-4}	2×10^{-4}	GE
423	50	8.4×10^{-4}	4×10^{-5}	4.5×10^{-2}	2×10^{-3}	GE
423	80	1.37×10^{-3}	6×10^{-5}	2.8×10^{-2}	2×10^{-3}	GE
423	100	1.73×10^{-3}	8×10^{-5}	2.3×10^{-2}	1×10^{-3}	GE
423	300	4.9×10^{-3}	2×10^{-4}	8.0×10^{-3}	6×10^{-4}	GE
423	500	7.8×10^{-3}	4×10^{-4}	5.0×10^{-3}	5×10^{-4}	GE
423	800	1.18×10^{-2}	5×10^{-4}	3.3×10^{-3}	4×10^{-4}	GE
423	1000	1.41×10^{-2}	8×10^{-4}	2.8×10^{-3}	4×10^{-4}	GE

Table S9: Computed compositions of $H_2O - H_2$ mixtures at coexistence using MC simulations. x_{H_2} is the mole fraction of hydrogen in the liquid phase, y_{H_2O} is the mole fraction of water in the gas phase. The $H_2O - H_2$ mixture is defined by the TIP5P/Ew[9]-Marx[22] force fields. σ_x is the uncertainty of x.

T/[K]	P/[bar]	x_{H_2}/[−]	$\sigma_{x_{H_2}}$	y_{H_2O}/[−]	$\sigma_{y_{H_2O}}$	Sim. Tech.
323	10	1.67×10^{-4}	8×10^{-6}	2.9×10^{-2}	2×10^{-3}	GE
323	50	8.5×10^{-4}	6×10^{-5}	6×10^{-3}	1×10^{-3}	GE
323	100	1.7×10^{-3}	1×10^{-4}	3.0×10^{-3}	6×10^{-4}	GE
323	300	4.9×10^{-3}	4×10^{-4}	1.4×10^{-3}	5×10^{-4}	GE
323	500	7.9×10^{-3}	8×10^{-4}	8×10^{-4}	4×10^{-4}	GE
323	800	1.2×10^{-2}	1×10^{-3}	6×10^{-4}	3×10^{-4}	GE
366	10	1.9×10^{-4}	1×10^{-5}	1.75×10^{-1}	7×10^{-3}	GE
366	50	2.34×10^{-3}	7×10^{-5}	2.27×10^{-2}	9×10^{-4}	GE
366	100	2.12×10^{-3}	9×10^{-5}	1.9×10^{-2}	1×10^{-3}	GE
366	300	6.1×10^{-3}	3×10^{-4}	6.8×10^{-3}	5×10^{-4}	GE
366	500	9.7×10^{-3}	5×10^{-4}	4.4×10^{-3}	4×10^{-4}	GE
366	800	1.42×10^{-2}	5×10^{-4}	2.9×10^{-3}	4×10^{-4}	GE
366	1000	1.73×10^{-2}	9×10^{-4}	2.4×10^{-3}	4×10^{-4}	GE
423	50	1.64×10^{-3}	6×10^{-5}	2.2×10^{-1}	1×10^{-2}	GE
423	100	3.6×10^{-3}	1×10^{-4}	1.14×10^{-1}	5×10^{-3}	GE
423	300	1.05×10^{-2}	3×10^{-4}	4.1×10^{-2}	2×10^{-3}	GE
423	500	1.65×10^{-2}	5×10^{-4}	2.6×10^{-2}	1×10^{-3}	GE
423	800	2.40×10^{-2}	8×10^{-4}	1.7×10^{-2}	1×10^{-3}	GE
423	1000	2.8×10^{-2}	1×10^{-3}	1.41×10^{-2}	7×10^{-4}	GE

Table S10: Parameters used for equation of state modeling: critical temperatures (T_c), pressures (P_c), and acentric factors (ω) the components at the standard reference state (1 bar).[38–40]

Component	T_c /[K]	P_c /[Pa]	ω
H_2	33.14	1296400	-0.219
H_2O	647.1	22064000	0.3443
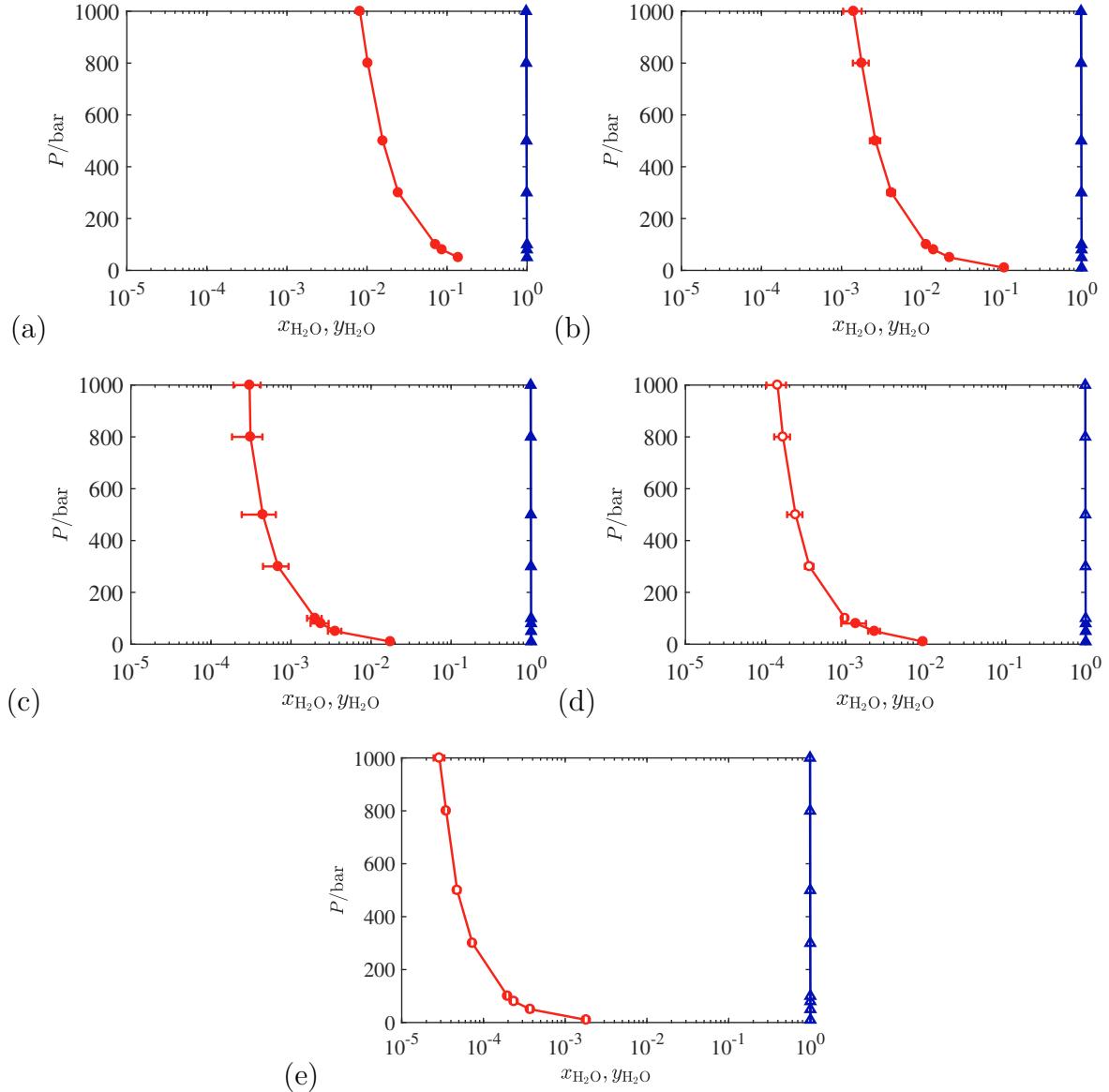
Figure S1: *P*-*x*-*y* phase diagrams of water-hydrogen (TIP3P[13]-Marx[22]) at pressures between 10 and 1000 bar and temperatures: (a) *T*=423 K, (b) *T*=366 K, (c) *T*=323 K, (d) *T*=310 K, (e) *T*=283 K. Dew points are denoted with circles and bubble points are denoted with triangles.

References

(1) Poursaeidesfahani, A.; Hens, R.; Rahbari, A.; Ramdin, M.; Dubbeldam, D.; Vlugt, T. J. H. Efficient application of Continuous Fractional Component Monte Carlo in the Reaction Ensemble. *J. Chem. Theory Comput.* **2017**, *13*, 4452–4466.

(2) Poursaeidesfahani, A.; Torres-Knoop, A.; Dubbeldam, D.; Vlugt, T. J. H. Direct Free Energy Calculation in the Continuous Fractional Component Gibbs Ensemble. *J. Chem. Theory Comput.* **2016**, *12*, 1481–1490.

(3) McQuarrie, D. A.; Simon, J. D. *Physical Chemistry: A Molecular Approach*, 1st ed.; University Science Books: Sausalito, California, 1997.

(4) Walas, S. M. *Phase Equilibria in Chemical Engineering*, 1st ed.; Butterworth-Heinemann: USA, 1985.

(5) Sandler, S. I. *Chemical, Biochemical, and Engineering Thermodynamics*, 4th ed.; John Wiley & Sons: USA, 2017.

(6) Lemmon, E. W.; Huber, M. L.; McLinden, M. O. NIST reference fluid thermodynamic and transport properties–REFPROP. *NIST standard reference database* **2002**, *23*, v7.

(7) Michelsen, M.; Mollerup, J. M. *Thermodynamic Models: Fundamental & Computational Aspects*, 2nd ed.; Tie-Line Publications: Holte, Denmark, 2007.

(8) Ángel Martín,; Bermejo, M. D.; Mato, F. A.; Cocero, M. J. Teaching advanced equations of state in applied thermodynamics courses using open source programs. *Educ. Chem. Eng.* **2011**, *6*, e114 – e121.

(9) Rick, S. W. A reoptimization of the five-site water potential (TIP5P) for use with Ewald sums. *J. Comput. Phys.* **2004**, *120*, 6085–6093.

(10) Allen, M. P.; Tildesley, D. J. *Computer simulation of liquids*, 2nd ed.; Oxford university press: Oxford, United Kingdom, 2017.

(11) Frenkel, D.; Smit, B. *Understanding molecular simulation: from algorithms to applications*, 2nd ed.; Academic Press: San Diego, California, 2002.

(12) Mark, P.; Nilsson, L. Structure and dynamics of the TIP3P, SPC, and SPC/E water models at 298 K. *J. Phys. Chem. A* **2001**, *105*, 9954–9960.

(13) Jorgensen, W. L.; Chandrasekhar, J.; Madura, J. D.; Impey, R. W.; Klein, M. L. Comparison of simple potential functions for simulating liquid water. *J. Chem. Phys.* **1983**, *79*, 926–935.

(14) Berendsen, H. J. C.; Grigera, J. R.; Straatsma, T. P. The missing term in effective pair potentials. *J. Phys. Chem.* **1987**, *91*, 6269–6271.

(15) Izadi, S.; Anandakrishnan, R.; Onufriev, A. V. Building Water Models: a different approach. *J. Phys. Chem. Lett.* **2014**, *5*, 3863–3871.

(16) Abascal, J. L. F.; Vega, C. A general purpose model for the condensed phases of water: TIP4P/2005. *J. Chem. Phys.* **2005**, *123*, 234505.

(17) Horn, H. W.; Swope, W. C.; Pitera, J. W.; Madura, J. D.; Dick, T. J.; Hura, G. L.; Head-Gordon, T. Development of an improved four-site water model for biomolecular simulations: TIP4P-EW. *J. Chem. Phys.* **2004**, *120*, 9665–9678.

(18) Buch, V. Path integral simulations of mixed para-D_2 and ortho-D_2 clusters: The orientational effects. *J. Chem. Phys.* **1994**, *100*, 7610–7629.

(19) Hirschfelder, C.; Curtiss, F.; Bird, R. B. *Molecular Theory of Gases and Liquids*; Wiley: New York, 1954.

(20) Köster, A.; Thol, M.; Vrabec, J. Molecular models for the hydrogen age: hydrogen, nitrogen, oxygen, argon, and water. *J. Chem. Eng. Data* **2018**, *63*, 305–320.

(21) Cracknell, R. F. Molecular simulation of hydrogen adsorption in graphitic nanofibres. *Phys. Chem. Chem. Phys.* **2001**, *3*, 2091–2097.

(22) Marx, D.; Nielaba, P. Path-integral Monte Carlo techniques for rotational motion in two dimensions: Quenched, annealed, and no-spin quantum-statistical averages. *Phys. Rev. A* **1992**, *45*, 8968–8971.

(23) Lemmon, E. W.; Span, R. Short fundamental equations of state for 20 industrial fluids. *J. Chem. Eng. Data* **2006**, *51*, 785–850.

(24) Lemmon, E. W.; Huber, M. L.; McLinden, M. O. NIST reference fluid thermodynamic and transport properties–REFPROP. *NIST standard reference database* **2002**, *23*, v7, `https://www.nist.gov/publications/nist-standard-reference-database-23-reference-fluid-thermodynamic-and-transport`, accessed 17/7/2019.

(25) Peng, D.-Y.; Robinson, D. B. A new two-constant equation of state. *Ind. Eng. Chem. Fundam.* **1976**, *15*, 59–64.

(26) Soave, G. Equilibrium constants from a modified Redlich-Kwong equation of state. *Chem. Eng. Sci.* **1972**, *27*, 1197 – 1203.

(27) Wagner, W.; Pruß, A. The IAPWS formulation 1995 for the thermodynamic properties of ordinary water substance for general and scientific use. *J. Phys. Chem. Ref. Data* **2002**, *31*, 387–535.

(28) Wiebe, R.; Gaddy, V. L. The solubility of hydrogen in water at 0, 50, 75 and 100° from 25 to 1000 atmospheres. *J. Amer. Chem. Soc.* **1934**, *56*, 76–79.

(29) Meyer, M.; Tebbe, U.; Piiper, J. Solubility of inert gases in dog blood and skeletal muscle. *Pflügers Archiv European Journal of Physiology* **1980**, *384*, 131–134.

(30) Gillespie, P. C.; Wilson, G. M. *Vapor-Liquid Equilibrium Data on Water-Substitue Gas Components*; 1980; pp RR_41, 1–34, `https://www.osti.gov/biblio/6782591`, accessed 17/7/2019.

(31) Kling, G.; Maurer, G. The solubility of hydrogen in water and in 2-aminoethanol at temperatures between 323 K and 423 K and pressures up to 16 M Pa. *Chem. Thermodynamics* **1991**, *23*, 531–541.

(32) Devaney, W.; Berryman, J. M.; Kao, P.-L.; Eakin, B. *High Temperature V-L-E Measurements for Substitute Gas Components*; 1978; pp 1–27.

(33) Jung, J. Loslichkeit von Kohlenmonoxid und Wasserstoff in Wasser zwisen 0 C und 300 C. Ph.D. thesis, RWTH Aachen, 1962.

(34) Ipatev, V.; Teodorovich, V. Equilibrium compositions of vapor-gas mixtures over solutions. *Zh. Obshch. Khim.* **1934**, *4*, 395–399.

(35) Ugrozov, V. V. Equilibrium compositions of vapor-gas mixtures over solutions. *Russian Journal of Physical Chemistry* **1996**, *70*, 1240–1241.

(36) Maslennikova, V. Y.; Goryunova, N.; Subbotina, L.; Tsiklis, D. The Solubility of Water in Compressed Hydrogen. *Russian Journal of Physical Chemistry* **1976**, *50*, 240–243.

(37) Bartlett, E. P. The concentration of water vapor in compressed hydrogen, Nitrogen and a mixture of these gases in the presence of condensed water. *Journal of the American Chemical Society* **1927**, *49*, 65–78.

(38) Yaws, C. L. *Thermophysical properties of chemicals and hydrocarbons*, 2nd ed.; Gulf Professional Publishing: Oxford, UK, 2014.

(39) Chase, M. W.; Curnutt, J.; Prophet, H.; McDonald, R.; Syverud, A. JANAF thermochemical tables, 1975 supplement. *J. Phys. Chem. Ref. Data.* **1975**, *4*, 1–176.

(40) Chase, M. W. NIST-JANAF Themochemical Tables, Fourth Edition. *J. Phys. Chem. Ref. Data* **1998**, *4*, 1–1951.